Lab on a Chip

Accepted Manuscript

RSC Publishing

www.rsc.org/loc

Registered Charity Number 207890

Cite this: DOI: 10.1039/c0xx00000x

www.rsc.org/xxxxxx

ARTICLE TYPE

Digital PCR on an integrated self-priming compartmentalization chip

Qiangyuan Zhu, Lin Qiu, Bingwen Yu, Yanan Xu, Yibo Gao, Tingting Pan, Qingchang Tian, Qi Song, Wei Jin, Qinhan Jin, Ying Mu*

Received (in XXX, XXX) Xth XXXXXXXXX 20XX, Accepted Xth XXXXXXXXX 20XX

DOI: 10.1039/b000000x

An integrated on-chip valve-free and power-free microfluidic digital PCR device is for the first time developed by making use of a novel self-priming compartmentalization and simple dehydration control to realize 'divide and conquer' for single DNA molecule detection. The high gas solubility of PDMS is exploited to provide the built-in power of self-priming so that the sample and oil are sequentially sucked into the device to realize sample self-compartmentalization based on surface tension. The lifespan of its self-priming capability was about two weeks tested using an air-tight packaging bottle sealed with a small amount of petroleum jelly, which is significant for practical platform. The SPC chip contains 5120 independent 5 nL microchambers, allowing the samples to be compartmentalized completely. Using this platform, three different abundance of lung cancer related genes are detected to demonstrate the feasibility and flexibility of the microchip for amplifying single nucleic acid molecule. For maximal accuracy, within less than 5% of the measurement deviation, the optimal number of positive chambers is between 400 and 1250 evaluated by the Poisson distribution, which means one panel can detect an average of 480 to 4804 template molecules. This device without world-to-chip connections eliminates the bondage of the complex pipeline control, and is an integrated on-chip platform, which would be a significant improvement to digital PCR automation and more user-friendly.

Introduction

As an increasingly familiar cousin of quantitative PCR, digital PCR is a promising method for determining target DNA copy number and absolute quantification. Digital PCR is of higher sensitivity and precision and less ambiguity than qPCR.[1, 2] The key to digital PCR is the partitioning of the diluted sample and reaction components into hundreds or thousands of reaction chambers so that researchers can get the absolute copies of DNA molecules. The measurement is accomplished by counting the number of positive partitions after endpoint PCR amplification.[3, 4] Digital PCR does not require scientists to compare an unknown to a standard, thus eliminating the need for a standard curve.[5] Since it was developed, digital PCR has been utilized in a wide range of biological research including detection of rare mutations,[6, 7] bacteria,[8, 9] copy number variation,[10, 11] genetic allelic imbalance,[12-14] single cell genomics,[15-18] as well as calibration for next-generation sequencing.[19]

Digital PCR was first demonstrated by using a 384-well plate on the basis of quantification of PCR.[1, 20, 21] Since then, a number of microsystems designed to perform digital PCR were developed, such as microfluidic formats,[15, 22-24] a spinning disk platform,[25] an emulsion PCR,[26-28] microdroplets,[29-37] and a slip-chip,[38, 39] which are summarized as digital PCR on chip or in droplets.[3] The reported chip for digital PCR, using integrated microvalves or micro-sized holes array, offers simple microchip device, but the chip needs mechanical connection to an external instrument. For example, many tubes for liquid transportation, syringe pumps for pressure-driven flow, and external air pressure for microvalves control.[22] Although droplet digital PCR methods can perform a large number of droplet reactions[40], it requires a complicated workflow consisting of microdroplets generator, droplet transfer, microplate sealing and droplet readout system.[29] These pieces of apparatus are often bulky and expensive. Therefore, the world-to-chip fluidic/electrical interconnections of digital PCR techniques are notoriously cumbersome. This limitation hinders maximum utilization of the benefits of microfluidic digital PCR platforms. The challenge is to develop a novel, compact, lower cost and all-on-chip format with all functions including the self-priming of the sample, the autonomous compartmentalization of partitioning the sample, and without complex control systems to meet the needs of the researchers.

The integrated all-on-chip digital PCR will be the future for the next generation digital PCR. To realize the combination of the all-in-chip for the digital PCR, better establish 'divide and conquer' for single DNA molecule detection, three key points must be taken into consideration. First, a built-in power source should be exploited to drive liquid flow into microwells of the chip. Second, each microwell was compartmentalized effectively with each other. Third, a single DNA molecule amplification should be ensured. Although a self-digitization chip has been reported based on viscoelastic fluid phenomena driven by the geometric properties of a microfluidic channel, there are many limitations.[41, 42] 1) The chip should be primed with an immiscible phase in advance. 2) Digitization worked adequately needs

certain fairly stringent geometric parameters. 3) This chip need connect with tubes and a compressor providing air pressure. 4) This chip has not been used to perform digital PCR.

Compared to self-digitization chip[43], our previous reported self-priming compartmentalization digital LAMP chip has many advantages[44]. Without valves, power, priming with an immiscible phase in advance and fairly stringent geometric parameters, there is no connection with tubes and compressor. The feature of the high gas solubility of PDMS was exploited to provide the power.[45-47] Air dissolved in PDMS can be evacuated by putting the PDMS chip in a vacuum, when the chip is brought back to the atmosphere, the ambient air will dissolve into the PDMS up to equilibrium. The re-dissolution of air through the microchannels walls provides a kinetic energy for the solution to move into the channel.[48] The pressure difference of the air dissolved in PDMS provides an inner power source so that sample solution and oil are sequentially sucked into the channels and microwells to realize 'divide and conquer' for single molecule amplification.

However, the self-priming compartmentalization digital LAMP chip can't be directly used to perform digital PCR. First, this chip can't effectively prevent from evaporation. Besides, in 95 ^{o}C denaturation temperature, the increases of the saturated vapor pressure of water caused the volume expansion, and the reaction reagents easily spilled from the microchambers to cause cross-reaction.

So, on the basis of our previous design, we made a lot of improvements. A serial of rectangular microwells connected with interlaced bifurcation channels and main channels are designed to realize sample partition. A mixed self-curing silicone oil was use in place traditional microvalves.[44] And, a low-permeability fluorosilane polymer was used to prevent the evaporation. Thus, in this paper, a novel integrated self-priming compartmentalization (SPC) on-chip digital PCR device was developed for the first time which was made mainly with PDMS and was vacuum packaged.

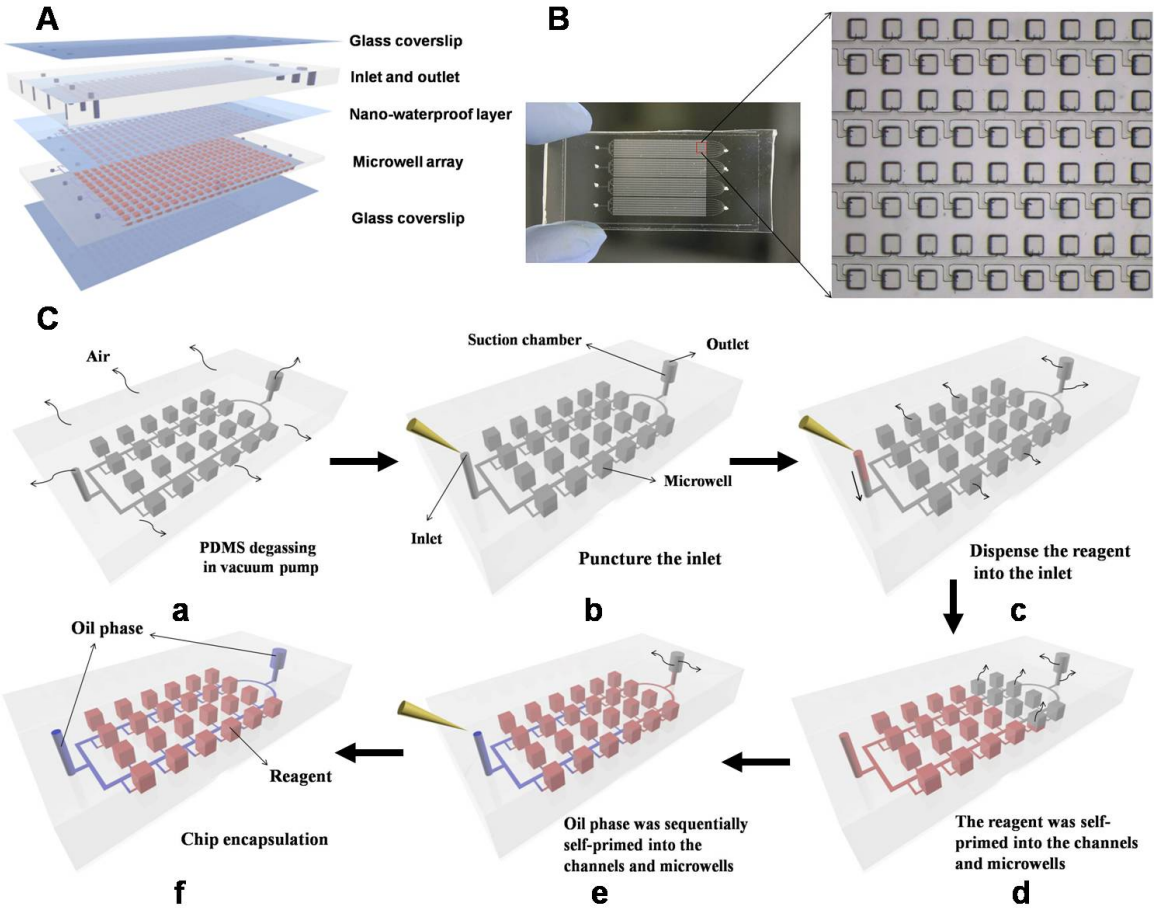

Fig. 1 Schematic drawing shows the design and mechanism of the microfluidic chip for the digital PCR. (A) Schematic diagram of the layered device structure of the microfluidic chip, which is composed of two layers of PDMS (an inlet and outlet layer and a flow layer containing hundreds of microwells), and nano-waterproof layer, bonding on a glass coverslip. (B) Photograph of the prototype device. It contains four separated panel, the blue lines are the flow channel. The red cuboids (150 mm × 150 mm × 250 mm) stand for the microwells. The size of the chip is 50 mm × 24 mm × 4 mm. (C) The principle and operation procedure of the self-priming compartmentalization microfluidic device: (a) Degassing of the microchip in a vacuum pump; an adhesive tape was attached after the degassing of the microchip and then storage at vacuum packaging; (b) The adhesive tape was punctured; (c) Dispensing of the reagent into the inlet; (d) Degassing-drive flow primes the sample into the microwells; (e) Dispensing the oil into the inlet, the oil phase was self-primed into the channels, and the sample solution in channels was partitioned individually into empty microwells left (extra sample was sucked into the suction chamber); and (f) All the microwells were partitioned by oil after the suction chamber was overfilled. The SPC chip was sealed by adhesive tape after the extra sample was pushed out of the suction chamber by oil phase.

Experimental

SPC Chip Design and Fabrication

The self-priming compartmentalization (SPC) microfluidic chips are fabricated with multilayer soft lithography techniques. The SPC chips were composed of three layers of the silicone elastomer polydimethylsiloxane (PDMS) bonded to a glass coverslip (0.17 mm) with an embedded fluorosilane polymer layer (supplementary Figure 1). The SPC chip patterns were designed using Corel DRAW X4 and printed on transparency films by a high resolution printer. First, the 4-inch silicon wafers were baked at 200 ^{o}C for 10 min to promote dehydration. The flow molds were prepared by spin-coating a photoresist (SU8-3025) onto silicon wafers (3000 rpm for 30 s) to create an approximately 25 μm high flow channel. According to manufacturer specifications, after the wafers were soft baked at 95 ^{o}C for 15 min, the channel patterns were exposed onto them by ultraviolet light with a mask aligner. Then the molds were put onto a hot plate (95 ^{o}C) for 40 min to perform post-bake. After that, the molds were developed and hard baked at 200 ^{o}C for 60 min to protect this layer during subsequent processing. When the flow channels were completed, SU8-2075 was utilized for the microwells fabrication. SU8-2075 was spin-coated (3000 rpm for 30 s) to a thickness of 75 μm on the flow channels. After soft baking, a second layer of SU8-2075 was spun (1000 rpm for 30 s) to the first layer. The features of the microwells on the masks should be aligned to the flow channels. After exposure and development of the two SU8-2075 layers, the microwells layer molds were defined. Finally, the molds were baked on a hotplate at 300 ^{o}C for 30 min to make the features hard for repeated use. The length and width of the rectangular microwell master molds were both 150 μm, of which the height was 250 μm.

The SPC devices were made from PDMS (GE RTV 615) which is a two component PDMS elastomer. The molds were treated with a vapor of trimethylchlorosilane for 1 min before use to prevent adhesion of PDMS. First, a 300 μm-thick thin layer was created by spincoating 5 A : 1 B (excess Si–H groups) mixture of PDMS on the mold at 1000 rpm for 30 s. After baking at 80 ^{o}C for 5 min, 10 nm-thick layer of low-permeability fluorosilane polymer was created by spinning electronic grade coating (EGC-1720, 3M) on the PDMS layer. The coating can dry immediately, then, 5 A : 1 B (excess Si–H groups) PDMS was poured on the coating layer. The top layer is cast thickly (4 mm) for mechanical stability to allow reliable use. Another blank 4 mm-thick PDMS was prepared on a clear wafer. After baking both molds on a hotplate at 80 ^{o}C for 45 min, the PDMS block on the fluid mold was peeled off to punch holes. Then the 4 mm-thick blank PDMS block was aligned to the outlet of microwell array layer to punch holes (2.5 mm in diameter) as the suction chambers, and the microwell array layer was sealed with a pretreated glass coverslip by plasma pre-treatment system. Finally, the suction chamber layer was bonded on the microwell layer and baking for 4 h at 80 ^{o}C on a hotplate.

Microchip Operation

First, the oil phase was prepared according to the following steps: the 1.1 g of uncured PDMS was mixed at the ratio of 10 A : 1 B in a 5 mL tube, then, 4 g of silicone oil (50 cst) was added to the uncured PDMS and mixed well by vortexing. Before being used, the mixed oil phase performed vacuum degassing. After that, the top surface of the SPC chip was pasted with a transparent adhesive tape, and then it was placed in the vacuum pump system to perform degassing. Air located in the PDMS was evacuated at 1 kPa for 20 min. Then, the microchip was taken out, and the transparent adhesive tape is punctured with a syringe needle. A 8.5 μL of sample solution was then dispensed via the sample injection port with a conventional micropipette. Sequentially, when the sample was totally sucked into the channels and chambers, the silicone oil was added in the injection port and was sucked into the channels following the sample solution with a clear contact line at the PDMS-oil-sample interface. When the samples were individually separated by oil into the microwells, the PDMS, which was previously mixed at the ratio of 10 A : 1 B, was dispensed into the inlets and outlets. At last, a glass coverslip was pressed on the upper surface of the SPC microchip without bubbles. So, the self-priming microchip was encapsulated into a whole set which was then ready to be used to perform subsequent digital PCR reaction.

Digital PCR

All reaction components, including the PCR master mix, primers, probe, and template were assembled and mixed off-chip before analysis with the SPC digital PCR chip. To minimize pipetting variability, all components were premixed before dispensing aliquots in different tubes and adding template solutions. The mix was supplemented with 0.1% TWEEN 20 to prevent reaction components from being adsorbed during the reaction. The SPC chip was tested with a sample containing 10^7 copies/μL DNA plasmids which was determined by its absorption at 260 nm. Then, the performance of the SPC chip was tested using the serial dilutions of the stock DNA solution at 4 orders of magnitude from 1 : 10^3, 1 : 10^4, 1 : 10^5 to 1 : 10^6. The reaction mix (20 μL) was prepared, comprising of 2×TaqMan® Gene Expression Master Mix 10 μL (Applied Biosystems, PN 4369016), forward primer 1 μL (10 nM), reverse primer 1 μL (10 nM), probe 1 μL (5 nM), RNase-free water 5 μL, 0.1% TWEEN-20 1 μL and serially diluted template 1 μL was prepared. A bench-top PCR machine (MGL96G, Long Gene) with a flat-bed heating block was used to carry out the digital PCR using the SPC device with mineral oil interfacing the block surface and the glass. The thermocycling protocol included a 2 min heating step at 50 ^{o}C , 10 min hot start at 95 ^{o}C; and then 40 cycles: 15 s at 95 ^{o}C; 1 min at 60 ^{o}C. The experiments were repeated three times to ensure the robustness and reproducibility of the SPC chip.

For the lung cancer related genes detection, 2×10^6 A549 cells in suspension were collected to extract total RNA using AxyPrep™ Multisource Total RNA Miniprep Kit (Axygen Biosciences). The total RNA was examined with spectrophotometer and electrophoresis, and then submitted to do cDNA synthesis (TaKaRa). The concentration of cDNA stock solution was measured spectrophotometrically and was serially diluted using RNase-free water, and the range of final template concentration in the PCR mixture was from 25 ngμL^{-1}, 2.5 ngμL^{-1}, 0.25 ngμL^{-1} to 0.025 ngμL^{-1}. The reaction mix (20 μL) for each digital panel comprises 2×TaqMan® Gene Expression Master Mix 10 μL, 20×TaqMan® Gene Expression Assay 1 μL (Applied Biosystems), RNase-free water 6μL, serially diluted template (cDNA) 1 μL, and 0.1% TWEEN-20 1 μL, Negative controls

contained RNase-free water in place of cDNA. The cycling program is 2 min at 50 °C; 10 minutes at 95 °C; and then 40 cycles: 15 seconds at 95 °C; 60 seconds at 60 °C. The real-time PCR of the same reaction components was performed for comparison with digital PCR using a 7900HT system (Applied Biosystems).

Data Acquisition and Analysis

The chip after amplification was detected using Maestro Ex IN-VIVO Imaging System (CRI Maestro). Fluorescence images were acquired by using a large area CCD system. An enlarged image can be observed by using fluorescence microscope (OLYMPUS). The fluorescence was excited at 455 nm and the emitted light was accepted by the CCD through a 495 nm long-pass filter. The ROX as the reference fluorescence was deducted as the background.

Results and discussions

Fabrication of Valve-free Chip and Principle of the Power-free Pumping

The microfluidic chip was designed with a series of rectangular microwells which were located on interlaced bifurcation channels comprised of eight main channels (2.5 cm in length and 25 μm in height). All ends of the 8 parallel flow channels are converged, respectively, to a sample injection port and a dynamic suction chamber. The diameter of the sample injection port is 0.5 mm, and a PDMS block with dynamic suction chamber was added to provide additional power to drive the flow. The diameter of suction chamber port is 2.5 mm. All the parts described above forms one individual reaction panel, and the microchip consists of four such panels which can detect 4 samples or replications of the same sample simultaneously. Each panel contains 1280 independent 5 nL microwells which allows a minimum sample of approximately 8.5 μL to be delivered into each microwell (Fig. 1 A, B). By experimental test, the 6.5 μL of samples was contained in the SPC chip. The uniformity of the compartmentalization was analyzed by fluorescent intensity. The variation of chamber volumes is about 9.4% (Notes S1).

The most outstanding feature of the microchip is its self-priming compartmentalization. Because of the air permeability of the PDMS, very little air exists in the bulk of the PDMS after being degassed. When placed in the atmosphere, difference of air pressure in and out of the bulk of the PDMS serves as the energy for sample and oil introduction sequentially like an embedded self-priming micropumps (Fig. 1C(a, b)). When the sample solution was dispensed on the injection port, it was, then, primed into microwells by the pressure difference (Fig. 1C(c, d)). Once the sample was completely primed into the microchip, the oil was dispensed into the same inlet. Once the oil sucked into the channel, it could then propel the sample in the main channel into the subsequent microwells which had not been full until all samples were driven into the empty wells. The sample solution was discretized automatically by the thousands of embedded self-priming micropumps (Fig. 1C(e)). When the sample solution was in excess of its allotted volume, the extra portion would be sucked into the suction chamber and be pushed out by the oil before the chip was sealed with a glass coverslip (Fig. 1C(f)). The details of self-priming compartmentalization of a solution were shown in Fig. 2. Compared to the self-digitization chip, our method is much simpler and more robust. During the driving of air pressure difference, the solution was priming into the microchambers without priming with an immiscible phase in advance. All empty microchambers quickly filled with the solution without any air bubbles within about 2 minutes (Fig. 2). The silicone oil was primed into the microchannels sequentially and made all the microchambers to be compartmentalized. This method did not depend on the fairly stringent geometric parameters, and there is no connection with tubes and compressor. What's more, another feature of the microchip is self-curing of oil phase during the thermocycling, so that the sample could be divided more effectively. Due to the silicone oil contains uncured PDMS polymers, so the oil phase can be cured by the elevated temperature during thermal cycling. In this way, thousands of independent partitions are created automatically without the need of any valves and outer power source making the microfluidic digital PCR chip work independently. Since the SPC chip consists of only two layers of PDMS and one cover-glass with no mechanical connection to any external tools, the only required manual operation is pipetting (Video S1).

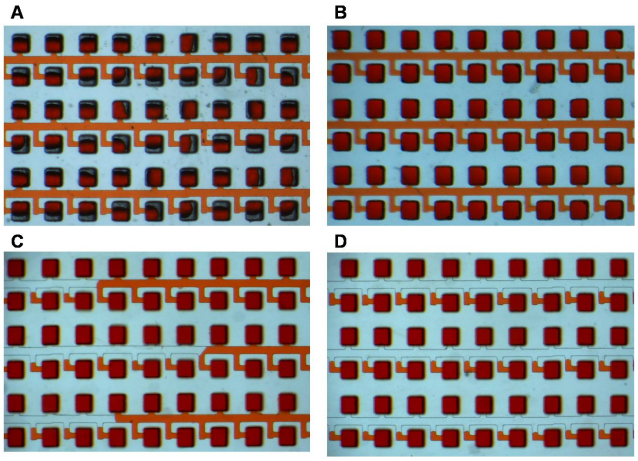

Fig. 2 Schematic drawings show the procedure of self-priming compartmentalization of an aqueous sample. (A) During the driving of air pressure, the aqueous was priming into the microchambers. (B) All the empty microchambers slowly filled with the solution. (C) The silicone oil was primed into the microchannels, and pushed the solution into the suction chambers. (D) All the microchambers were compartmentalized.

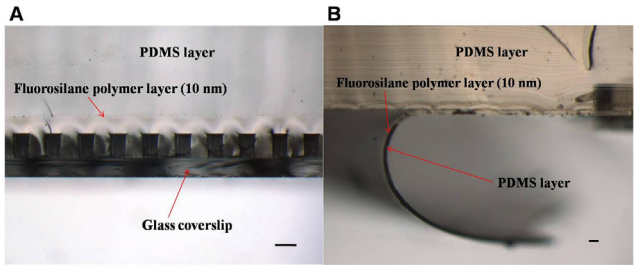

Fig. 3 Scheme of nano-waterproof layer embedded in SPC chip. (A) A complete microchip fabrication process was described with an embedded nano-waterproof layer made of fluorosilane polymer (10 nm). (B) Cross-section of the SPC digital PCR microchip. The array layer was located between the glass coverslip and the fluorosilane polymer layer (10 nm) which stopped from water evaporation. Scale bar is 200 μm. (C) Optical micrograph describing the structure of the fluorosilane polymer layer bonding with PDMS during a peal test. Scale bar is 500 μm.

Dehydration of Digital PCR Reaction

Although gas solubility of PDMS provides power for sample partition, it also lead to water evaporation and vapor transportation during thermocycling, a problem that is exacerbated in reactors with high surface-to-volume ratio (S/V; ~ 3.3×10^4 m^{-1}). To resolve these competing requirements, a novel ~10 nm-thick layer of low-permeability fluorosilane polymer embedded ~ 50 μm above the digital PCR array was introduced (Fig. 3 and Notes S2). This layer sealing the top of the array creates an effective permeation barrier, thereby restricting vapor transport within a thin slab of PDMS that becomes saturated after the evaporation of only a small fraction of the reaction volumes. The maximum fractional loss of water from the reaction chambers is: 2.88%, and this amount of water loss does not inhibit PCR amplification and is much less than the water loss caused by the integrated Parylene C membrane. Compared to the procedure of integration of the parylene C layer, the workflow of this method is exceedingly simple.[22] The coating was spin-coated on the PDMS layer and dried in seconds, and then the uncured PDMS was poured on the film to form a PDMS-fluorosilane polymer-PDMS hybrid after being thermally cured. The water vapor gradients at the periphery of the array are controlled by the inclusion of hydration lines (100 μm × 100 μm) to enable robust single-DNA-molecule amplification.

Determining DNA copy number by digital PCR

By mathematical analysis,[49-51] the maximum theoretical dynamic range of the designed SPC digital PCR can detect 6210 molecules (Notes S3 and Fig. S2). To test the digital PCR response on the SPC chip, a tenfold serial dilution of the β-actin DNA stock solution was prepared at 4 orders of magnitude from 1 : 10^3 to 1 : 10^6 and from 0.7 cpw (copy per microwell) to 0.001 cpw. Each pre-mixed solution injected into the chip contained 1 μL of diluted DNA template solution, then, the mixed solution was evenly distributed into three panels of the same chip. For the same concentration, the experiment was repeated three times. At this concentration, the average template number of the individual microwells was expected to be no more than one molecule, and a color image of digital PCR on the microchip with concentrations of *β*-actin DNA was taken by the Maestro Ex IN-VIVO Imaging System (Fig. 4A). As the concentration of the template DNA was diluted, the fraction of positive wells decreased as expected. At higher DNA titers, DNA samples should be serially diluted to prevent each microwell from capturing more than one copy of the template, as it would result in the measurement uncertainty.[52] An image of fluorescence intensity taken by the MATLAB analysis demonstrates that the fluorescence intensity in the positive microchambers increased observably compared to the negative microchambers (Fig. S1). The results proved the feasibility of the SPC digital PCR for single nucleic acid amplification.

When single DNA molecules are randomly partitioned into these chambers, it is possible that two or more molecules are present in the same chamber. The probability increases as the number of molecules per panel (or DNA concentration) increases. As a result there may be more molecules in each panel than there are calls. Therefore, Random and independent distribution of target DNA molecules throughout partitions is critical to accurate digital PCR detection.[22]

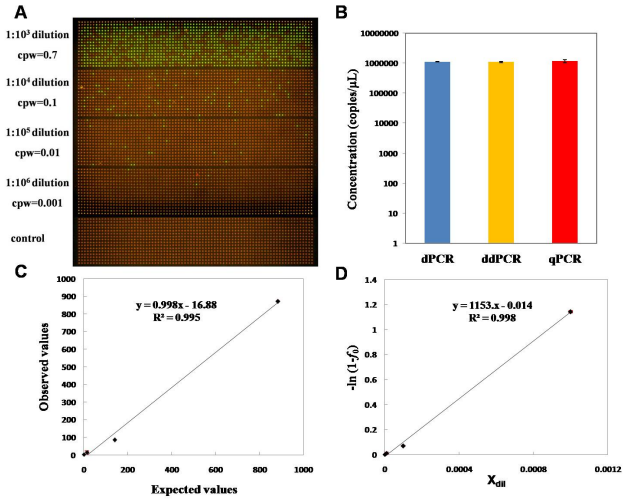

Fig. 4 Digital PCR results on the SPC microchip. (A) Digital PCR with a serial dilution of target DNA template ranging from 1 : 10^3 to 1 : 10^6 dilutions. At low template concentrations, DNA molecules can be counted absolutely. There is no positive signal in control when no target DNA template was loaded. (B) Comparison of quantitative real-time PCR, droplet digital PCR and SPC digital PCR quantification results of copy number for *β*-actin gene. (C) The copy number of the templates can be calculated from the number of positive microwells. The observed positive microwells match well with the predicted values according to Poisson statistics (R^2= 0.995). (D) A regression curve was acquired by plotting the -ln(1- f_0) against the dilution factor Xdil, which is the linear form of the Poisson distribution equation. According to the equation, the copy number of the stock solution of DNA can be calculated.

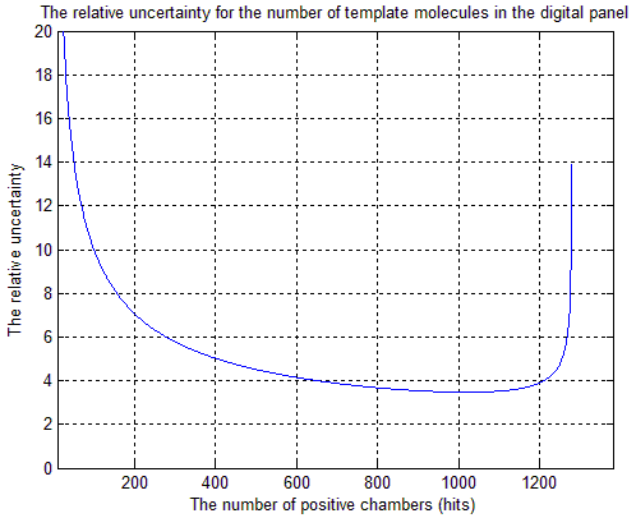

Fig. 5 Graph showing the relationship of the relative measurement uncertainty and the number of positive chambers (hits). One can infer that a wide range of number of hits from 400 to 1250 gives smallest possible uncertainty in the estimation of the concentration of the gene permitting the 95% confidence interval.

A mathematical correction of the Poisson distribution can be applied to calculate DNA templates permitting the mathematical correction in 95% confidence interval estimation background (Notes S4, S5).[53] The calculation is derived from the total number of chambers in the panel and the number of detected calls. The result demonstrated that the observed number of the positive chambers has good correlation with the expected number of the

positive chambers (R^2 = 0.995), which was calculated according to the Poisson distribution (Fig. 4C). Then, a regression curve was acquired by plotting -ln(1- f_0) against the dilution factor X_{dil}, which is the linear form of the Poisson distribution.[34] The initial concentration of the DNA stock solution from the linear regression fit was determined (Fig. 4D). Fig. 4B shows a linear regression fit to the four concentrations in the dilution series, yielding a value of a stock concentration of $c_0 = (1.12 \pm 0.01) \times 10^6$ copies per μL. Compared this result with conventional real-time quantitative PCR, as indicated in Fig. 4B, the concentration was measured to be $(1.16 \pm 0.14) \times 10^6$ copies per μL. We also use Bio-Rad droplet digital PCR to detect the sample, yielding a stock concentration of the $c_0 = (1.09 \pm 0.06) \times 10^6$ copies per μL (Fig. 4B). As shown in the graph, the results of the SPC and the commercial droplet digital PCR match closely. The result of qPCR has the maximal error of more than 14%. The results demonstrated that the chip developed could produce robust results which follow the Poisson distribution (Table S1).

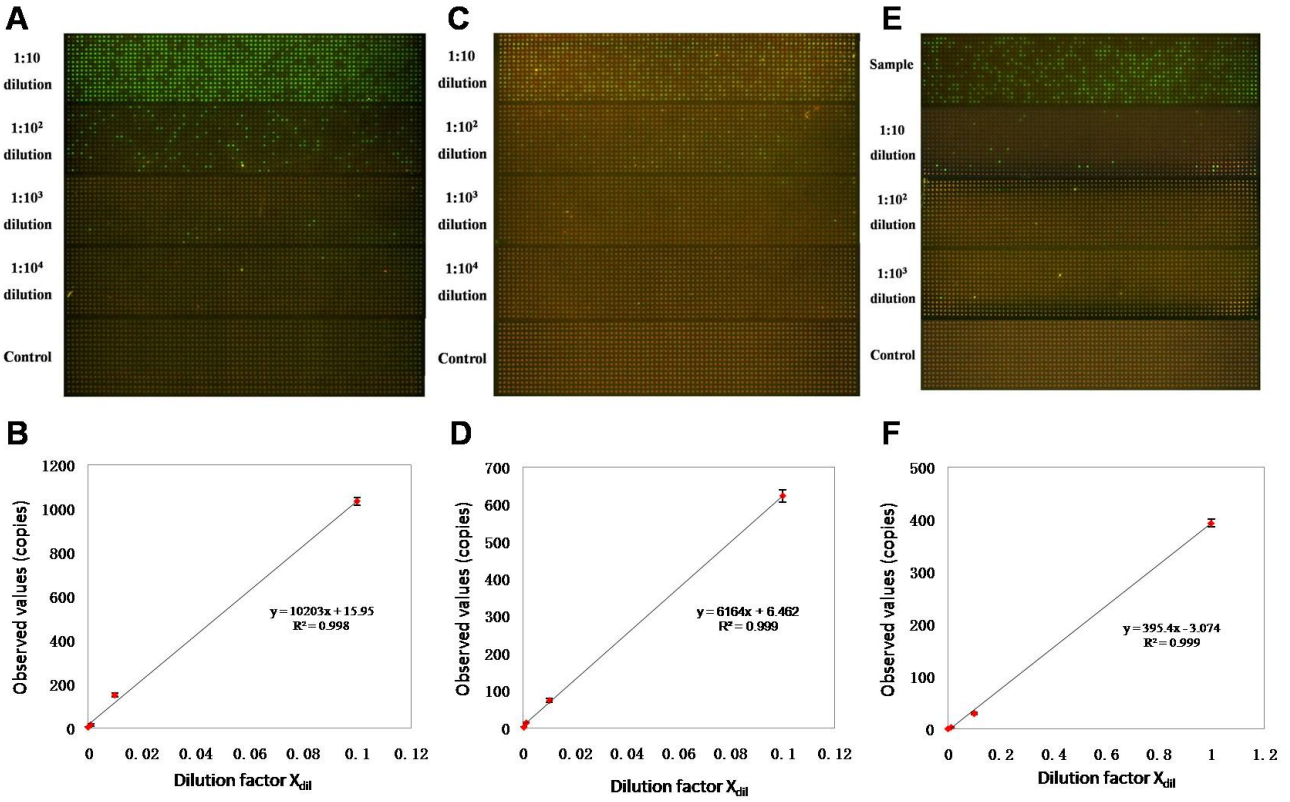

Fig. 6 Quantifications of copy number of four genes at varying dilution concentrations using the SPC digital PCR microchip. (A) Digital PCR fluorescent imagines of PLAU with a serial dilution of target DNA template. There is no positive signal in control. (B) A regression curve of PLAU was acquired by plotting the observed positive points against the dilution factor X_{dil}. (C) Digital PCR fluorescent imagines of ENO2 with a serial dilution of target DNA template. (D) A regression curve of ENO2 was acquired by plotting the observed positive points against the dilution factor X_{dil}. (E) Digital PCR fluorescent imagines of PLAT with a serial dilution of target DNA template. (F) A regression curve of PLAT was acquired by plotting the observed positive points against the dilution factor X_{dil}. The copies of the templates can be calculated from the number of positive microwells.

Measurement uncertainty of digital PCR

The measurement uncertainty in estimation of the number of template molecules per panel incorporates a component due to variance in the number of positive partitions following random distribution of a fixed number of target molecules and the stochastic component associated with the number of template molecules that are dispensed into the panel from a highly diluted PCR solution (Note S6 and Fig. S3).[54-56] The uncertainty for the number of template molecules per panel is related to both the number of chambers analyzed and the number of positive chambers. By mathematical analysis for the SPC digital PCR chip, the optimal number of positive chambers is 1024, the measurement uncertainty is about 3.5% (Fig. 5). Within less than 5% of the measurement deviation, the optimal number of positive chambers is between 400 and 1250. For maximal accuracy, it is recommended that each panel contains between 400 and 1250 positive microchambers, which means one panel contains an average of 480 to 4804 template molecules (Fig. 5).

In order to validate the SPC digital chip's ability to detect genome samples, and test the measurement uncertainty of the chip. Three different abundance of lung cancer related genes (PLAU, ENO2, PLAT) were detected by the SPC digital PCR. A curve is made to relate the fraction of the positive chambers (f_0) to the dilution factor X_{dil}. There was a linear variation of the fraction of the positive chambers with 4 DNA template concentrations (R^2_{PLAU}=0.998, R^2_{ENO2}=0.999, R^2_{PLAT}=0.999). The relative uncertainty which is within 5.0% is 1.6%, 0.6% and 1.3% (Fig. 6). The raw statistical data are included in the electronic supplemental information (Tables S2, S3). As shown in Fig. 7, from the low copy samples to the high copy samples, the quantitative results about different abundance of genes is within the 95% confidence interval. Compared this result with real-time quantitative PCR, as shown in Fig. 8, the SPC digital PCR has the

samller measurement uncertainty and better reliability. Therefore, the chip could be used to determine the absolute DNA concentration precisely.

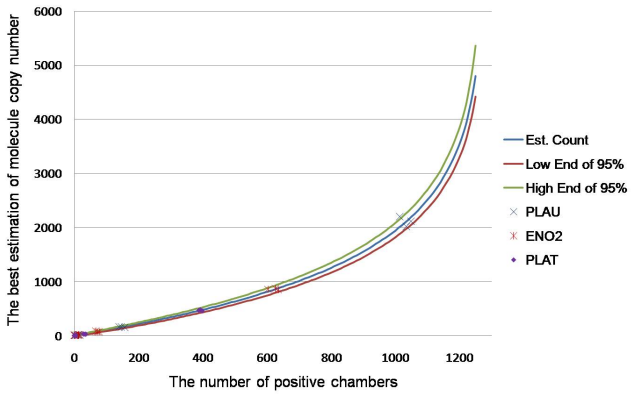

Fig. 7 Graph showing the relationship of the relative measurement uncertainty and the number of positive chambers (hits). One can infer that a wide range of number of hits from 400 to 1250 gives smallest possible uncertainty in the estimation of the concentration of the gene permitting the 95% confidence interval.

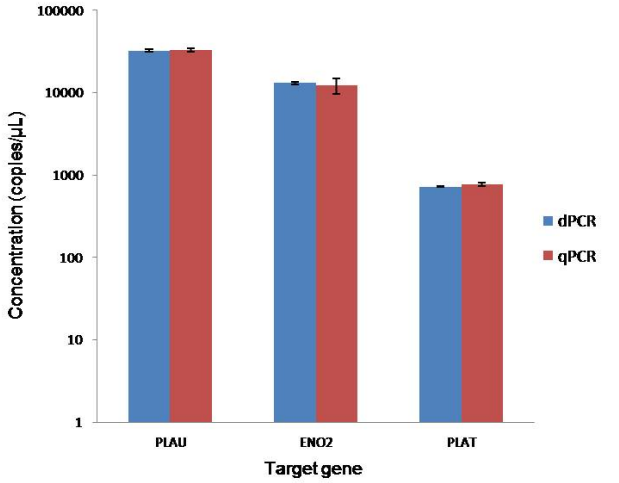

Fig. 8 Comparison of real-time quantitative PCR and digital PCR quantification results of copy number for three different abundance of lung cancer related genes (PLAU, ENO2, PLAT).

Conclusions

The novel fluorosilane polymer was employed to prevent the dehydration of nanolitre volume PCR reaction. The coating dries to a thin, optically transparent, non-flammable, permanent film with excellent hydrophobic and oleophobic properties. It can adhere to a variety of surfaces including glass, metals and metal oxides. Without activating the surface of the fluorosilane polymer, it can directly bond with the PDMS. Due to the coating being spun onto the thin microwells PDMS layer directly, fabrication difficulties in transferring the membrane were avoided, the PDMS slab defined by the glass substrate and the integrated fluorosilane polymer membrane was also much thinner. Therefore, thickness of the PDMS between the top of the chamber and the fluorosilane polymer membrane was only designed to be 50 μm which is thin enough to ensure minimal evaporation of PCR reaction mixtures during thermocycling. This method of preventing evaporation has the advantages of simple in fabrication, convenient in operation, etc. It would be an excellent method to prevent and control evaporation for all kinds of microfluidic devices.

In order to increase measurement precision, sensitivity, and dynamic range of the digital PCR measurement, a higher reaction chamber density and scale of the SPC digital PCR device was developed. This device would enable digital PCR in an inexpensive, high-performance, and high throughput format. Using the optimized multilayer soft lithography fabrication process some super-density SPC digital PCR arrays of AZ4620 photoresist features. The arrays have dimensions of 4 x 4 x 10 μm on an 8 μm pitch, corresponding to sub-pL chambers (160 fL) with a density of 1,562,500 / cm^2, and a scale of approximately 6,000,000 reactions per device have been made. Although soft lithography has been shown capable of reproducing smaller scale features, the observed microwells having minimum dimensions of less than ~2 μm are prone to collapse, likely due to surface tension effects. When the devices are degassed in a vacuum, the microwells are even more prone to collapse. Thus, it is estimated that smaller chamber size is not appropriate to be fabricated using PDMS. For digital PCR to be competitive against qPCR, the cost and throughput of each device should also be taken into consideration. Taking the SPC chip of 6,000,000 reactions as an example, the chip could be configured to have 600 samples x 10,000 chambers to meet the most of the applications.

The self-priming capability of the SPC chip is up to the seal or the vacuum retention. The self-priming capability of the chip sealed with transparent adhesive tape could last for approximately 4 h. The lifespan of its self-priming capability was tested using an air-tight packaging bottle sealed with a small amount of petroleum jelly. The self-priming capability of the chip can last for two weeks, which is significant for practical issues. It may be an important step to move the microfluidic devices beyond laboratory setting. If excellent air tightness measures were employed, looks like vacuette blood collection tube, the self-priming capability of the chip would be able to last for a longer time. The longer lasting chip will have more outstanding application merits in biological fields. As long as there is a SPC chip and a bench-top PCR machine with a flat-bed heating block, researchers will be able to perform digital PCR without specialized training (Fig. S4). If the SPC digital PCR chip is integrated with the potable heating system[57] and imaging system[58], such as an infrared heating[59] or a mobile phone[60, 61], the SPC digital PCR device will become an all-on-chip system, which is enough for point-of-care testing[62]. Taking all these advantages of on-chip and high density features into consideration, it is foreseeable that the SPC chip would provide a valuable platform for digital PCR and make it become one of the most useful tools in life science fields including early diagnosis of cancer, non-invasive prenatal diagnosis, single cell analysis and single cell genomics sequencing, etc. [63, 64]

Acknowledgement

This work was supported by the National Natural Science Foundation of China (31070772, 31270907), the National Basic Research Program of China (2007CB714500), and the State Key

Laboratory of Industrial Control Technology, Zhejiang University, China. The authors would like to thank Dr. Jiang Huang's kind help on chip fabrication technique and Dr. Xuguang Zhu's kind comments on article construction and word polishing.

Notes and references

Research Center for Analytical Instrumentation, Institute of Cyber-Systems and Control, State Key Laboratory of Industrial Control Technology, Zhejiang University, Hangzhou, P. R. China. Fax: +86 571-88208382; Tel: +86 571-88208383; E-mail: muying@zju.edu.cn

† Electronic Supplementary Information (ESI) available: [details of any supplementary information available should be included here]. See DOI: 10.1039/b000000x/

1. B. Vogelstein and K. W. Kinzler, *Proc. Natl. Acad. Sci. USA*, 1999, **96**, 9236-9241.
2. N. Blow, *Nat. Methods*, 2007, **4**, 869-875.
3. M. Baker, *Nat. Methods*, 2012, **9**, 541-544.
4. G. Pohl and L. M. Shih, *Expert Rev. Mol. Diagn*, 2004, **4**, 41-47.
5. A. S. Whale, J. F. Huggett, S. Cowen, V. Speirs, J. Shaw, S. Ellison, C. A. Foy and D. J. Scott, *Nucleic Acids Res.*, 2012, **40** (11): e82.
6. T. K. F. Yung, K. C. A. Chan, T. S. K. Mok, J. Tong, K. F. To and Y. M. D. Lo, *Clin. Cancer Res.*, 2009, **15**, 2076-2084.
7. J. Wang, R. Ramakrishnan, Z. Tang, W. W. Fan, A. Kluge, A. Dowlati, R. C. Jones and P. C. Ma, *Clin. Chem.*, 2010, **56**, 623-632.
8. E. A. Ottesen, J. W. Hong, S. R. Quake and J. R. Leadbetter, *Science*, 2006, **314**, 1464-1467.
9. A. D. Tadmor, E. A. Ottesen, J. R. Leadbetter and R. Phillips, *Science*, 2011, **333**, 58-62.
10. R. Chen, G. I. Mias, J. Li-Pook-Than, L. H. Jiang, H. Y. K. Lam, E. Miriami, K. J. Karczewski, M. Hariharan, F. E. Dewey, Y. Cheng, M. J. Clark, H. Im, L. Habegger, S. Balasubramanian, M. O'Huallachain, J. T. Dudley, S. Hillenmeyer, R. Haraksingh, D. Sharon, G. Euskirchen, P. Lacroute, K. Bettinger, A. P. Boyle, M. Kasowski, F. Grubert, S. Seki, M. Garcia, M. Whirl-Carrillo, M. Gallardo, M. A. Blasco, P. L. Greenberg, P. Snyder, T. E. Klein, R. B. Altman, A. J. Butte, E. A. Ashley, M. Gerstein, K. C. Nadeau, H. Tang and M. Snyder, *Cell*, 2012, **148**, 1293-1307.
11. J. Qin, R. C. Jones and R. Ramakrishnan, *Nucleic Acids Res.*, 2008, **36** (18): e116.
12. Y. M. D. Lo, F. M. F. Lun, K. C. A. Chan, N. B. Y. Tsui, K. C. Chong, T. K. Lau, T. Y. Leung, B. C. Y. Zee, C. R. Cantor and R. W. K. Chiu, *Proc. Natl. Acad. Sci. USA*, 2007, **104**, 13116-13121.
13. H. C. Fan, Y. J. Blumenfeld, U. Chitkara, L. Hudgins and S. R. Quake, *Proc. Natl. Acad. Sci. USA*, 2008, **105**, 16266-16271.
14. H. C. Fan, Y. J. Blumenfeld, Y. Y. El-Sayed, J. Chueh and S. R. Quake, *Am. J. Obstet. Gynecol.*, 2009, **200** (5): 543. e1-7.
15. L. Warren, D. Bryder, I. L. Weissman and S. R. Quake, *Proc. Natl. Acad. Sci. USA*, 2006, **103**, 17807-17812.
16. T. Kalisky and S. R. Quake, *Nat. Methods*, 2011, **8**, 311-314.
17. V. Sanchez-Freire, A. D. Ebert, T. Kalisky, S. R. Quake and J. C. Wu, *Nat. Protoc.*, 2012, **7**, 829-838.
18. A. K. White, K. A. Heyries, C. Doolin, M. Vaninsberghe and C. L. Hansen, *Anal. Chem.*, 2013, **85**, 7182-7190.
19. R. A. White, P. C. Blainey, H. C. Fan and S. R. Quake, *BMC. Genomics*, 2009, **10**, 116.
20. P. J. Sykes, S. H. Neoh, M. J. Brisco, E. Hughes, J. Condon and A. A. Morley, *Biotechniques*, 1992, **13**, 444-449.
21. O. Kalinina, I. Lebedeva, J. Brown and J. Silver, *Nucleic Acids Res.,* 1997, **25**, 1999-2004.
22. K. A. Heyries, C. Tropini, M. VanInsberghe, C. Doolin, O. I. Petriv, A. Singhal, K. Leung, C. B. Hughesman and C. L. Hansen, *Nat. Methods*, 2011, **8**, 649-651.
23. F. M. F. Lun, R. W. K. Chiu, K. C. A. Chan, T. Y. Leung, T. K. Lau and Y. M. D. Lo, *Clin. Chem.*, 2008, **54**, 1664-1672.
24. Y. F. Men, Y. S. Fu, Z. T. Chen, P. A. Sims, W. J. Greenleaf and Y. Y. Huang, *Anal. Chem.*, 2012, **84**, 4262-4266.
25. S. O. Sundberg, C. T. Wittwer, C. Gao and B. K. Gale, *Anal. Chem.*, 2010, **82**, 1546-1550.
26. F. Diehl, M. Li, Y. P. He, K. W. Kinzler, B. Vogelstein and D. Dressman, *Nat. Methods*, 2006, **3**, 551-559.
27. M. Li, F. Diehl, D. Dressman, B. Vogelstein and K. W. Kinzler, *Nat. Methods*, 2006, **3**, 95-97.
28. D. Dressman, H. Yan, G. Traverso, K. W. Kinzler and B. Vogelstein, *Proc. Natl. Acad. Sci. USA*, 2003, **100**, 8817-8822.
29. R. Tewhey, J. B. Warner, M. Nakano, B. Libby, M. Medkova, P. H. David, S. K. Kotsopoulos, M. L. Samuels, J. B. Hutchison, J. W. Larson, E. J. Topol, M. P. Weiner, O. Harismendy, J. Olson, D. R. Link and K. A. Frazer, *Nat. Biotechnol.*, 2009, **27**, 1025-1031.
30. N. R. Beer, B. J. Hindson, E. K. Wheeler, S. B. Hall, K. A. Rose, I. M. Kennedy and B. W. Colston, *Anal. Chem.*, 2007, **79**, 8471-8475.
31. N. R. Beer, E. K. Wheeler, L. Lee-Houghton, N. Watkins, S. Nasarabadi, N. Hebert, P. Leung, D. W. Arnold, C. G. Bailey and B. W. Colston, *Anal. Chem.*, 2008, **80**, 1854-1858.
32. H. Song, D. L. Chen and R. F. Ismagilov, *Angew. Chem. Int. Edit.*, 2006, **45**, 7336-7356.
33. P. Kumaresan, C. J. Yang, S. A. Cronier, R. G. Blazej and R. A. Mathies, *Anal. Chem.*, 2008, **80**, 3522-3529.
34. L. Mazutis, A. F. Araghi, O. J. Miller, J. C. Baret, L. Frenz, A. Janoshazi, V. Taly, B. J. Miller, J. B. Hutchison, D. Link, A. D. Griffiths and M. Ryckelynck, *Anal. Chem.*, 2009, **81**, 4813-4821.
35. B. J. Hindson, K. D. Ness, D. A. Masquelier, P. Belgrader, N. J. Heredia, A. J. Makarewicz, I. J. Bright, M. Y. Lucero, A. L. Hiddessen, T. C. Legler, T. K. Kitano, M. R. Hodel, J. F. Petersen, P. W. Wyatt, E. R. Steenblock, P. H. Shah, L. J. Bousse, C. B. Troup, J. C. Mellen, D. K. Wittmann, N. G. Erndt, T. H. Cauley, R. T. Koehler, A. P. So, S. Dube, K. A. Rose, L. Montesclaros, S. L. Wang, D. P. Stumbo, S. P. Hodges, S. Romine, F. P. Milanovich, H. E. White, J. F. Regan, G. A. Karlin-Neumann, C. M. Hindson, S. Saxonov and B. W. Colston, *Anal. Chem.*, 2011, **83**, 8604-8610.
36. M. M. Kiss, L. Ortoleva-Donnelly, N. R. Beer, J. Warner, C. G. Bailey, B. W. Colston, J. M. Rothberg, D. R. Link and J. H. Leamon, *Anal. Chem.*, 2008, **80**, 8975-8981.
37. H. F. Zhang, G. Jenkins, Y. Zou, Z. Zhu and C. J. Yang, *Anal. Chem.*, 2012, **84**, 3599-3606.
38. F. Shen, W. B. Du, J. E. Kreutz, A. Fok and R. F. Ismagilov, *Lab. Chip*, 2010, **10**, 2666-2672.
39. F. Shen, W. B. Du, E. K. Davydova, M. A. Karymov, J. Pandey and R. F. Ismagilov, *Anal. Chem.*, 2010, **82**, 4606-4612.
40. A. C. Hatch, J. S. Fisher, A. R. Tovar, A. T. Hsieh, R. Lin, S. L. Pentoney, D. L. Yang and A. P. Lee, *Lab. Chip*, 2011, **11**, 3838-3845.

41. D. E. Cohen, T. Schneider, M. Wang and D. T. Chiu, *Anal. Chem.*, 2010, **82**, 5707-5717.
42. T. Schneider, G. S. Yen, A. M. Thompson, D. R. Burnham and D. T. Chiu, *Anal. Chem.*, 2013, **85**, 10417-10423.
43. A. Gansen, A. M. Herrick, I. K. Dimov, L. P. Lee and D. T. Chiu, *Lab. Chip*, 2012, **12**, 2247-2254.
44. Q. Y. Zhu, Y. B. Gao, B. W. Yu, H. Ren, L. Qiu, S. H. Han, W. Jin, Q. H. Jin and Y. Mu, *Lab. Chip*, 2012, **12**, 4755-4763.
45. K. Hosokawa, K. Sato, N. Ichikawa and M. Maeda, *Lab. Chip*, 2004, **4**, 181-185.
46. K. Hosokawa, M. Omata, K. Sato and M. Maeda, *Lab. Chip*, 2006, **6**, 236-241.
47. K. Hosokawa, M. Omata and M. Maeda, *Anal. Chem.*, 2007, **79**, 6000-6004.
48. I. K. Dimov, L. Basabe-Desmonts, J. L. Garcia-Cordero, B. M. Ross, Y. Park, A. J. Ricco and L. P. Lee, *Lab. Chip*, 2011, **11**, 4279-4279.
49. S. Dube, J. Qin and R. Ramakrishnan, *Plos One*, 2008, **3** (8): e2876.
50. S. L. Spurgeon, R. C. Jones and R. Ramakrishnan, *Plos One*, 2008, **3** (2): e1662.
51. L. B. Pinheiro, V. A. Coleman, C. M. Hindson, J. Herrmann, B. J. Hindson, S. Bhat and K. R. Emslie, *Anal. Chem.*, 2012, **84**, 1003-1011.
52. A. S. Whale, S. Cowen, C. A. Foy and J. F. Huggett, *Plos One*, 2013, **8** (3): e58177.
53. R. Sanders, J. F. Huggett, C. A. Bushell, S. Cowen, D. J. Scott and C. A. Foy, *Anal. Chem.*, 2011, **83**, 6474-6484.
54. K. R. Griffiths, D. G. Burke and K. R. Emslie, *Anal. Methods*, 2011, **3**, 2201-2211.
55. S. Bhat, J. Herrmann, P. Armishaw, P. Corbisier and K. R. Emslie, *Anal. Bioanal. Chem.*, 2009, **394**, 457-467.
56. A. Chunovkina and A. Chursin, *S. Adv. Math.*, 2001, **57**, 55-66.
57. H. Kim, S. Vishniakou and G. W. Faris, *Lab. Chip*, 2009, **9**, 1230-1235.
58. R. D. Stedtfeld, D. M. Tourlousse, G. Seyrig, T. M. Stedtfeld, M. Kronlein, S. Price, F. Ahmad, E. Gulari, J. M. Tiedje and S. A. Hashsham, *Lab. Chip*, 2012, **12**, 1454-1462.
59. Y. Yu, B. Li, C. A. Baker, X. Zhang and M. G. Roper, *Anal. Chem.*, 2012, **84**, 2825-2829.
60. H. Y. Zhu, S. Mavandadi, A. F. Coskun, O. Yaglidere and A. Ozcan, *Anal. Chem.*, 2011, **83**, 6641-6647.
61. H. Y. Zhu, O. Yaglidere, T. W. Su, D. Tseng and A. Ozcan, *Lab. Chip*, 2011, **11**, 315-322.
62. C. J. Easley, J. M. Karlinsey, J. M. Bienvenue, L. A. Legendre, M. G. Roper, S. H. Feldman, M. A. Hughes, E. L. Hewlett, T. J. Merkel, J. P. Ferrance and J. P. Landers, *Proc. Natl. Acad. Sci. USA*, 2006, **103**, 19272-19277.
63. F. McCaughan and P. H. Dear, *J. Pathol.*, 2010, **220**, 297-306.
64. E. Day, P. H. Dear and F. McCaughan, *Methods*, 2013, **59**, 101-107.